Inorganic Chemistry Communications 132 (2021) 108846

Contents lists available at ScienceDirect

Inorganic Chemistry Communications

journal homepage: www.elsevier.com/locate/inoche

Design, synthesis and investigation of procaine based new Pd complexes as DNA methyltransferase inhibitor on gastric cancer cells

Salih Paşa [a], Omer Erdogan [b], Ozge Cevik [b,*]

[a] Afyon Kocatepe University, Faculty of Education, Department of Science, Afyonkarahisar 03200, TURKEY
[b] Aydin Adnan Menderes University, School of Medicine, Department of Biochemistry, Aydin 09010, TURKEY

ARTICLE INFO

Keywords:
Procaine
Schiff Ligand
Pd Complex
DNMT Inhibitor
Anticancer
Apoptosis

ABSTRACT

Procaine is a specific inhibitor of DNA methyltransferase (DNMT). In the present work, the Schiff base ligands were synthesized from procaine with the addition of salicylaldehyde and naphthaldehyde as metal precursor for procaine-based transition metal complexes ($\mathbf{L^1}$ and $\mathbf{L^2}$) with palladium (Pd). The compounds were checked and characterized for identity and purity using elemental analysis, SEM, melting points, FT-IR, and NMR spectral data. Among the compounds, $\mathbf{L^1}$**-Pd** and $\mathbf{L^2}$**-Pd** were found to display significant cytotoxicity with IC_{50} values of 10.21 μM and 10.79 μM against human gastric cancer cell line MKN-45. Novel synthesized procaine derivatives target molecules and their palladium complexes had an inhibitory effect on colony formation and wound healing on MKN-45 cells. Furthermore, these compounds were evaluated for their apoptotic activity and DNMT activity in MKN-45 cells. Western blotting and qPCR studies demonstrated that compound $\mathbf{L^1}$**-Pd** and $\mathbf{L^2}$**-Pd** induced apoptosis and a slight decrease in anti-apoptotic Bcl-2 protein/gene expression and highly increased pro-apoptotic Bax protein/gene expression in MKN-45 cells treated. Also, total DNMT enzyme activity and protein expression (DNMT1, DNMT3a, and DNMT3b) levels were decreased in $\mathbf{L^1}$**-Pd** and $\mathbf{L^2}$**-Pd** treated cells. The $\mathbf{L^1}$**-Pd** and $\mathbf{L^2}$**-Pd** complexes showed that they are potential new DNMT inhibitors to prevent cancer-induced DNA hypermethylation and can be used in the treatment of gastric cancer.

1. Introduction

Cancer is a brutal disease that is caused by several structural deteriorations at the cellular level. There are still no effective treatments for several types of cancer, however much research has been done to provide a greater understanding of the processes involved in the progression of the disease. Cancer cells have the ability to grow rapidly and form colonies or tumors within the living tissue. The colony formation assay has been the standard procedure to assess the effects of cytotoxic agents on cancer cells [1]. In addition to that, wound healing assay is a simple, inexpensive and effective method for monitoring the migration of cells. This method is constructed to observe cell migration into a "wound" that is created on a cell monolayer [2]. Advanced abilities such as invasion, migration, survival, and colony formation are required in the metastasis of cancer cells. The main handicap for cancer treatments is the lack of protection of the healthy cells in the body. Besides, the chemotherapy drugs are also highly toxic to normal cells, not specifically to cancer cells. Drugs synthesized to interrupt the various cancer mechanisms are more effective and attempts in this direction have rapidly gained momentum in recent years. As a result, many different investigations and approaches are now being used to develop new therapeutics.

DNA methyltransferase (DNMT) inhibitors are chemical components for hypomethylation of genome in multiple processes of DNA methylation (e.g., DNA imprinting and X-chromosome inactivation) and have recently been used as anticancer treatments [3–6]. DNMT enzymes may cause epigenetic modifications in the modulation of gene expressions by catalyzing some regions of DNA methylation. To date, three different DNMT (DNMT1, DNMT3a, and DNMT3b) that are responsible for the methylation of mammalian cells have been found. Essentially, most DNMTs have the capacity of catalyzing the addition of a methyl group to the fifth carbon atom of the cytosine residues at the CpG sites by using S-adenosyl methionine as a methyl donor [7]. The control of the DNMTs is crucial since the hypermethylation of tumor suppressor genes creates an aggressive process for cancer formation. Therefore, one of the approaches for cancer treatments is the development of DNA methyltransferase inhibitors. Procaine, azacytidine, decitabine, zebularine, etc., are currently used as DNMT inhibitors for cancer treatment. Due to

* Corresponding author.at: Aydin Adnan Menderes University, School of Medicine, Department of Biochemistry, Efeler, Aydin 09100, TURKEY.
E-mail address: ozge.cevik@adu.edu.tr (O. Cevik).

https://doi.org/10.1016/j.inoche.2021.108846
Received 21 April 2021; Received in revised form 1 August 2021; Accepted 4 August 2021
Available online 8 August 2021

the lack of data on many aspects of DNMT inhibitors a great deal of effort has been devoted to develop DNMT inhibitors for both specific cancers and for cancer in general [8]. DNMT inhibitors are generally classified into two different classes: nucleoside inhibitors and non-nucleoside inhibitors [9]. Nucleoside inhibitors are a class of nucleoside analogues that consist of cytidine derivatives which can be incorporated into DNA and can be effective by the formation of a suicidal covalent complex with DNMT. Non-nucleoside molecules are classified as compounds that have different chemical structures, these molecules generally bind directly to DNMT and result in changes in the mechanism of their actions [9]. Furthermore, DNA methylation is a stable epigenetic mark in humans since it takes place at the C5 location of cytosines, especially in a CpG dinucleotide context and in non-CpG regions of stem cells [10–12]. However, the use of these DNMT inhibitors is limited due to their disadvantages, such as poor structural stability, relative toxicity, and drug resistance [13]. Therefore, it is necessary to develop new DNMT inhibitors in cancer treatment.

Transition metals, called as d-block elements, are essential for many biological functions. Properties such as electron mobility in the valance shells and the ability to be coordinated by many ligands having electron donor elements, such as N, O, and S, makes them important in the areas of protein structural stability and functionality. In particular, palladium and platinum complexes such as cisplatin [14–16], have found a great deal of use as actual or potential anticancer agents.

In the current study, the effort has been made to enlighten the employment of Pd complexes, obtained from procaine-derived Schiff compounds, in DNA methylation to repress cancer growth. Procaine-originated structures have been frequently used for this purpose and attract great attention to be as a significant agent in DNMT inhibitors [17–22]. Therefore, ligands were selected from the previous studies [23,24] to investigate the best biological effect with their Pd complexes on Gastric Cancer Cells. The possible synergetic effect comprised of the Schiff base ligands ($\mathbf{L^1}$ and $\mathbf{L^2}$) and their transition metal complexes as $\mathbf{L^1}$**-Pd** and $\mathbf{L^2}$**-Pd** with the employment of procaine hasn't been investigated for DNMT inhibitors yet. Therefore, this work focuses on DNMT investigations with the newly synthesized Pd complexes containing Schiff base ligands to develop alternative drugs for gastric cancer treatments.

2. Experimental

2.1. Reagents and methods

All the reagents, solvents, and materials were commercially purchased from Sigma-Aldrich and Merck. The compounds and solvents were appropriately purified, if necessary. All cell culture supplements and medium for cell culture studies were purchased from Gibco Company. ^{13}C NMR and ^{1}H NMR spectra were recorded for obtained ligands and complexes in d_6-DMSO solution on a Bruker DPX 400 MHz spectrometer at 300 K. The morphological analyses were investigated by SEM-EDX (Scanning Electron Microscope-Energy Dispersive X-ray Spectroscopy) with LEO 1430 VP instrument working with tungsten filament lamp. The SEM images were recorded after 5000 times magnification. The stretching vibrations were obtained after 30 scans with 4 cm^{-1} resolution by Shimadzu LabSolutions IR 8000 with KBr pellet in the scale of 400–4000 cm^{-1}.

2.2. Synthesis of ligands and Pd(II) complexes

$\mathbf{L^1}$**:** *2-(diethylamino) ethyl 4-((2-hydroxybenzylidene) amino) benzoate*: The synthesis of $\mathbf{L^1}$ was performed according to the literature [23]. A procaine solution (0.236 g, 1 mmol) was dissolved properly in 30 mL ethanol in two necked round bottom flask. The salicylaldehyde (0.122 g, 1 mmol) was then diluted in 20 mL ethanol to add into the flask drop by drop. It was continued stirring for 3 h. The resulting yellow solid was filtered off and respectively washed with 10 mL cold ethanol and cold water. Yellow product was recrystallized in ethanol. The obtained precipitate was recovered by filtration, washed and air-dried. (Fig. 1) M.P: 170–174 °C, Yield: 93%. Elemental Analysis: [$C_{20}H_{24}N_2O_3$] (340.42 g/mol): C, 70.56; H, 7.11; N, 8.23; O, 14.10. IR(cm^{-1}, KBr): 1616 HC = N, 3406O-H, 1112 ArC-N, 3051 Ar-CH, 2976 Aliph-CH, 1712C = O, 1274C-O, 2484 hydroxyl stretching bond [25], 2582 atmospheric CO_2 [26]. ^{1}H NMR (DMSO-d_6): δ 9.02 ppm (1H, s, C***H*** = N), δ 1.27 ppm (6H, t, J = 8 Hz, N-(CH_2-C***H***$_3$)$_2$), δ 3.37 ppm (4H, q, J = 12 Hz, N-(C***H***$_2$-CH_3)$_2$), δ 4.52 ppm (4H, t, J = 4 Hz, –C***H***$_2$-C***H***$_2$–), δ 12.61 ppm (1H, s, –O***H***), δ 6.57–7.70 ppm (8H, m, Ar-C***H***). ^{13}C NMR (DMSO-d_6): δ 160 ppm (1H, ***C***H = N), δ 161 ppm (1H, Ar-***C***-OH), δ 9 ppm (N-(CH_2-***C***H_3)$_2$), δ 49 ppm (N-(***C***H_2-CH_3)$_2$), δ 58 ppm (O-CH_2-***C***H_2-N), δ 59 ppm (O-***C***H_2-CH_2-N), δ 165 ppm ***C*** = O), δ 117–136 ppm (Ar-**C**).

$\mathbf{L^2}$**:** *2-(diethylamino) ethyl 4-(((2-hydroxynaphthalen-1-yl)methylene) amino) benzoate*: The synthesis of L^2 was performed according to the literature procedure [24]. A solution of 2-hydroxynapthaldehyde (0.172 g, 1 mmol) in 30 mL ethanol and a solution of procaine (0.236 g, 1 mmol) in 30 mL ethanol were mixed and refluxed for 6 h. After the mixture was cooled to 25 °C, the solvents (EtOH and occurred water) were evaporated. The remained yellowish solid precipitate was recrystallized in ethanol. Then it was filtered and washed. It was yielded approximately 88% after dried in a ventilated oven. (Fig. 2) M.P: 183–185 °C, [$C_{24}H_{26}N_2O_3$] (390.47 g/mol): C, 73.82; H, 6.71; N, 7.17; O, 12.29. IR(cm^{-1}, KBr): 1624 HC = N, 3406O-H, 1153 ArC-N, 3057 Ar-CH, 2976 Aliph-CH, 1714C = O, 1271C-O. ^{1}H NMR (DMSO-d_6): δ 9.68 ppm (1H, s, C***H*** = N), δ 1.28 ppm (6H, t, J = 8 Hz, N-(CH_2-C***H***$_3$)$_2$), δ 3.24 ppm (4H, q, J = 4 Hz, N-(C***H***$_2$-CH_3)$_2$), δ 4.62 ppm (4H, –C***H***$_2$-C***H***$_2$–), δ 10.81 ppm (1H, s, –O***H***), δ 6.98–8.96 ppm (m, Ar-C***H***). ^{13}C NMR (DMSO-d_6): δ 154 ppm (1H, ***C***H = N), δ 172 ppm (1H, Ar-***C***-OH), δ 8 ppm (N-(CH_2-***C***H_3)$_2$), δ 47 ppm (N-(***C***H_2-CH_3)$_2$), δ 49 ppm (O-CH_2-***C***H_2-N), δ 50 ppm (O-***C***H_2-CH_2-N), δ 165 ppm ***C*** = O), δ 122–138 ppm (Ar-**C**).

$\mathbf{L^1}$**-Pd:** The ligand ($\mathbf{L^1}$, 0.0357 g, 0.105 mmol) was first dissolved in acetone:chloroform (10 mL + 10 mL) mixture by heating. A solution of palladium acetate ($Pd(AcO)_2$, 0.0112 g, 0.05 mmol) in 15 mL acetone was added dropwise into ligand solution. The reflux reaction was continued for 12 h. Subsequently, it was cooled to room temperature and the solvent was evaporated. Brown solid product was separated and washed with distilled water and ethanol. Then it was used without further purification. (Fig. 3) M.P: >250 °C. Yield: 71%. Elemental Analysis: [$C_{40}H_{46}N_4O_6Pd$] (785.24 g/mol): C, 61.18; H, 5.90; N, 7.14; O, 12.23; Pd, 13.55. IR(400–4000 cm^{-1}, KBr): 1600 HC = N, 1178 ArC-N, 3032 Ar-CH, 2916 Aliph-CH, 1716C = O, 1274C-O, 2848 symmetric CH_2 stretching transition [27], 464 Pd-O, 582 Pd-N. ^{1}H NMR (DMSO-d_6): δ 8.32 ppm (C***H*** = N), δ 1.23 ppm (N-(CH_2-C***H***$_3$)$_2$), δ 3.35 ppm (N-(C***H***$_2$-CH_3)$_2$), δ 4.40 ppm (–C***H***$_2$-C***H***$_2$–), δ 7.14–8.22 ppm (Ar-C***H***).

$\mathbf{L^2}$**-Pd:** A solution of ligand ($\mathbf{L^2}$, 0.0488 g, 0.05 mmol) in 20 mL ethanol was set in a reflux system. 0.0056 g, 0.025 mmol $Pd(AcO)_2$ was dissolved in 15 mL acetone and added drop by drop into the reaction flask. The reaction was refluxed for 12 h and subsequently cooled to room temperature. The evaporating solvents from the reaction mixture afforded a dark brown solid precipitate. It was washed with plenty of ethanol and distilled water to purify it from the unreacted compounds. The solid product was then dried and used without further purifications. (Fig. 4) M.P: >250 °C, Yield: 68%. [$C_{48}H_{50}N_4O_6Pd$] (885.35 g/mol): C, 65.12; H, 5.69; N, 6.33; O, 10.84; Pd, 12.02. IR(400–4000 cm^{-1}, KBr): 1600 HC = N, 1269 ArC-N, 3053 Ar-CH, 2918 Aliph-CH, 1716C = O, 1269C-O, 472 Pd-O, 592 Pd-N, 2848 symmetric CH_2 stretching transition [27]. ^{1}H NMR (DMSO-d_6): δ 8.70 ppm (C***H*** = N), δ 1.23 ppm (N-(CH_2-C***H***$_3$)$_2$), δ 3.31 ppm (N-(C***H***$_2$-CH_3)$_2$), δ 4.60 ppm (–C***H***$_2$-C***H***$_2$–), δ 6.11–8.26 ppm (m, Ar-C***H*** and napht.–C***H***).

2.3. Cell culture

MKN-45 human gastric cancer cell lines were used in this study. Cells were cultured in RPMI-1640 medium supplemented with 10% fetal bovine serum FBS, 100 U/mL penicillin and 100 μg/mL streptomycin

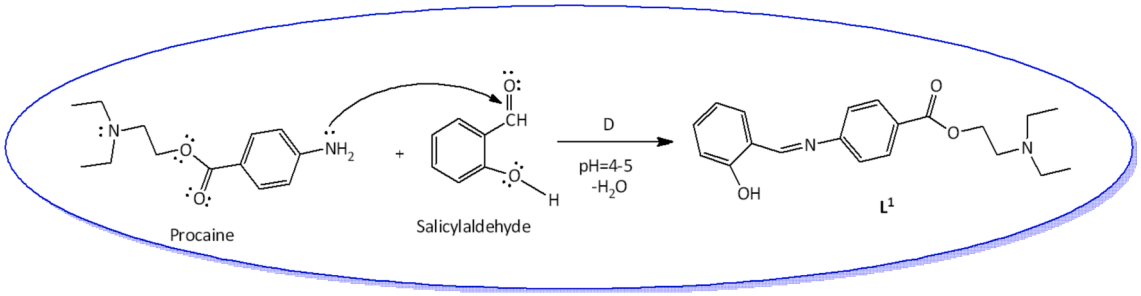

Fig. 1. The synthetic route of L^1 by condensation with procaine and salicylaldehyde.

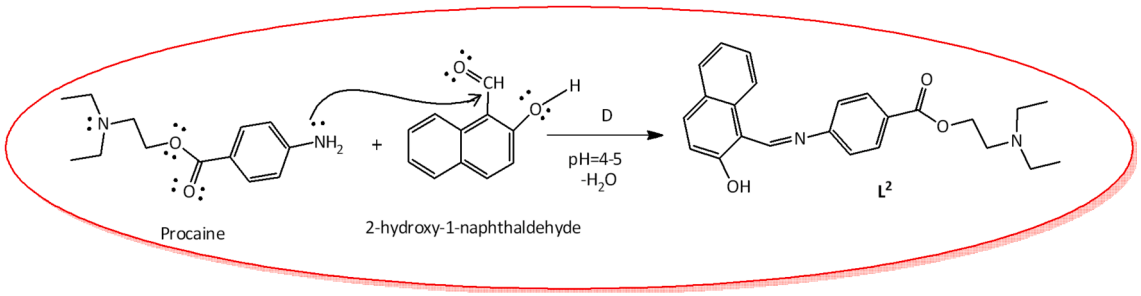

Fig. 2. The synthetic route of L^2 by condensation with procaine and 2-hydroxy-1-naphthaldehyde.

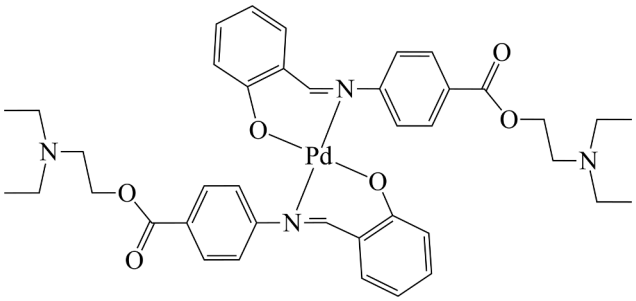

Fig. 3. The structural illustration of L^1-Pd complex.

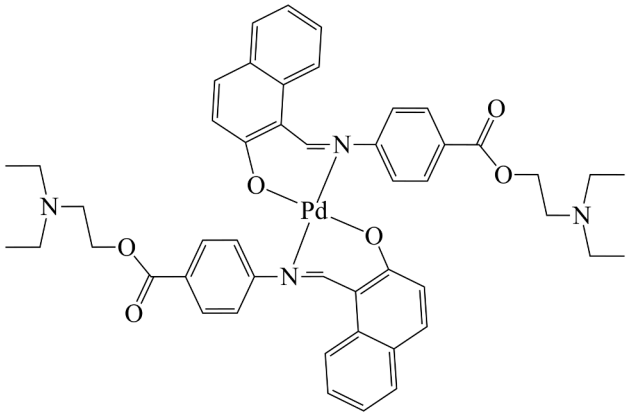

Fig. 4. The structural illustration of L^2-Pd complex.

and 2 mM L-glutamine. The cultures were incubated at 37C in a humidified atmosphere with 5% CO_2. The culture medium was replaced with fresh medium every 2 days until reaching suitable confluency of about 90%. All experiments were repeated multiple times.

2.4. Cell viability assay

The effects of procaine derivatives and their palladium complexes on MKN-45 cells viability were determined using a tetrazolium-based microplate assay with MTT, which was previously applied in our study. [28]. Briefly, the MKN-45 cells were seeded into a 96-well plate at a density of 1×10^4 cells/well in the 100 μL medium. After incubating the cells for 24 h, the dilutions of procaine derivatives and its palladium complexes at different doses (0.1–100 μg/mL) were added and incubated for 24 h. The percentage of cell viability was measured on ELISA reader (Biotek Co., USA) at a wavelength of 570 nm. The % cell viability was calculated using the formula given below in Eq. (1). The images of MKN-45 cells before and after treatment of procaine derivatives and its palladium complexes were also assessed using an inverted microscope attached to the camera system (Olympus NP40).

% Cell Viability= (OD test sample/OD control) X 100 (1)

2.5. Colony formation assay

The colony formation experiment was conducted according to the literature [29,30]. IC_{50} doses of procaine Pd complexes were added and incubated with MKN-45 cells for 24 h. After treatment, the medium containing procaine derivatives and its palladium complexes was removed and replaced with a pure medium. The medium was changed every 3 days for 10 days until visible colonies were formed. The stained cells were examined with an inverted microscope (Olympus CX40, Japan) and an imaging system. The number of colonies in each well was counted and analyzed [29,30].

2.6. Wound healing assay

The wound healing process was carried out according to the literature [31]. Cells were treated with procaine derivatives and its palladium complexes for 24 h. After an incubation period of 24 h, the cells migrated into the scratched area were photographed under a phase-contrast inverted microscope (Olympus CX40, Japan). The distance that cells had migrated into the cell-free space was measured by Image J software (NIH, USA). The width of each migrated area was used to calculate the

relative proportion of wounded at time zero [31].

2.7. Western blotting for protein expression

Bax, Bcl-2, DNMT1, DNMT3a and DNMT3b protein expression were determined with western blotting. For this purpose, the procedures worked before were followed [29,32,33]. The total proteins were extracted from $5x10^6$ cells that had been treated with procaine derivatives and its palladium complexes. The protein concentrations of lysates were determined by the bicinchoninic acid method (71285-Merck Millipore, Germany) [34]. Equal amount of protein was separated by 12% polyacrylamide gels and then transferred onto PVDF membranes (sc-3723, Santa Cruz, USA). The membranes were blocked with 2.5% BSA at 4C overnight and then incubated with specific primary antibodies (Bax (sc-7480), Bcl-2 (sc-492), DNMT1(sc-271729), DNMT3a (sc-373905), DNMT3b (sc-376043) and β-actin (sc-47778) from Santa Cruz Biotechnology, USA. After washing with Tris-buffered saline with 0.1% Tween-20 (TBST), the membranes were incubated with the corresponding HRP-conjugated secondary antibodies in room temperature. β-actin was used as a housekeeping control for normalization. The expression levels of proteins were visualized with an imaging system (SynGene G-BOX Chemi XRQ) and analyzed using the software.

2.8. QPCR for gene expression

The total RNA was extracted from $5x10^6$ MKN-45 cells as previously described [35]. A total of 1 μg RNA was reverse transcribed as the template for cDNA synthesis using high capacity cDNA Reverse Transcription Kit (Applied Biosytem). Quantitative real-time PCR was performed for Bax, Bcl-2 and GAPDH using primers. The primers sequence was: Bax: 5′-GCCCTTTTGCTTCAGGGTTT-3′(forward),5′-TCCAATGTCCAGCCCATGAT-3′(reverse); Bcl-2: 5′-GACAGAAGATCATGCCGTCC-3′(forward), 5′-GGTACCAATGGCACTTCAAG-3′(reverse); GAPDH: 5′-AGGGCTGCTTTTAACTCTGT-3′(forward), 5′-CCCCACTTGATTTTGGAGGA-3′(reverse). One hundred nanograms of cDNA were amplified using Sybr Green PCR Master Mix (Applied Biosytem) on the ABI StepOne Plus detection system, programmed for 95 °C for 10 min, then 40 cycles of: 95 °C for 15 s, 60 °C for 1 min. The amplification results were analyzed using StepOne Software v2.3 (Applied Biosystems, Foster City, CA) and the genes of interest were normalized to the corresponding GAPDH results. Data were expressed as fold induction relative to the control.

2.9. DNMT activity assay

The impact of the procaine derivatives and their palladium complexes on the methylation level was evaluated in MKN-45 gastric cancer cells using a colorimetric DNMT activity assay. Cells ($1x10^6$ cells/well) were seeded into a 60 mm culture dish and were allowed to grow overnight. Then, cells were treated with IC_{50} doses of procaine derivatives and its palladium complexes during 24 h. After incubating the cells for 24 h, cells were washed with 1x PBS solution and collected via trypsin. Nuclear extracts from cells were isolated using a commercial kit (Nuclear Extraction Kit 2900, Millipore). These extracts were then used for DNMT activity measurement. Experiments were carried out according to the commercial kit (DNMT Activity Quantification Kit ab113467, Abcam).

2.10. Statistical analysis

Data from three independent experiments are presented as mean ± SD. Differences between groups were analyzed by *t*-test of results. Statistical analysis was performed using GraphPad Prism version 5.0 software. Statistical significance is defined as follows: *, $p \leq 0.05$; **, $p \leq 0.01$; ***, $p \leq 0.001$.

3. Results and discussion

3.1. Chemical identification

The ^{1}H NMR spectra of $\mathbf{L^1}$ and $\mathbf{L^2}$ showed expected signals for the imine group (CH = N) at 9.02 ppm for $\mathbf{L^1}$ and 9.68 ppm for $\mathbf{L^2}$ [36]. These peaks in the L^1-Pd and L^2-Pd complexes have changed to 8.32 ppm and 8.70 ppm, respectively, as a result of coordination via the imine nitrogen atoms [37]. Signals due the hydroxyl protons, observed at 6.10 ppm and 6.08 ppm for the free ligands, disappeared on complexation, indicating deprotonation of the ligands. Peaks for the aliphatic and aromatic protons were also shifted upon complexation (Supplementary Material Figs. 1-8).

The infrared spectra show vibrations for three significant groups: imine (CH = N), metal–ligand (Pd-N, Pd-O) and hydroxyl (O-H). It was found that CH = N stretching vibrations of the ligands have been shifted to lower frequency in the complexes, as a consequence of coordination between the Pd and the imine nitrogen. The newly observed peaks at 582 cm^{-1} and 592 cm^{-1} correspond to Pd-N stretching vibrations. The absence of broad hydroxyl stretching (O-H) in the complexes, found at around 3200 cm^{-1} and 3400 cm^{-1} in the ligands, confirms the coordination between the metal atom and deprotonated oxygen atom [38]. The Pd-O vibrations were found at 464 cm^{-1} and 472 cm^{-1} [37–43].

The surface morphology (SEM images) of L^1-Pd and L^2-Pd looks like agglomerated particles (Fig. 5a) with stacked layers and small spherical particles, respectively (Supplementary Material Fig. 9-10). The elemental mapping images (Fig. 5a and Fig. 5b) of procaine Schiff-based Pd complexes clearly showed that both of the newly obtained compounds have Pd metals in their structure.

3.2. Effects of procaine derivatives on cell viability

The cytotoxic efficiencies of the compounds were investigated against MKN-45 gastric cancer cell lines and IC_{50} values were evaluated. The 50% inhibitory concentrations (IC_{50}) were determined after 24-hour exposure to 0.1–100 μM doses of procaine derivatives and the palladium complexes, and those concentrations (IC_{50}) were used in subsequent experiments. Treatment of MKN-45 gastric cancer cells with procaine derivatives and the palladium complexes inhibited the proliferation of the cells (Fig. 6). By looking at the morphological images of the MKN-45 cells (Fig. 6a), it was observed that the cells treated with procaine, L^1, L^1-Pd, L^2, and L^2-Pd demonstrated the signs of apoptosis, with the blebbing of the plasma membrane and reduction in cell size. On the other hand, especially the L^1-Pd and L^2-Pd compounds at IC_{50} doses, the cells moved away from each other and floated in the medium by rising from the well surface [44,45]. The IC_{50} concentrations of L^1-Pd and L^2-Pd complexes against the MKN-45 cells were calculated as 10.21 ± 2.21 and 10.79 ± 1.48, respectively. Tanaka et al. reported IC_{50} doses of glycoconjugated palladium complexes on MKN-45 and MKN-28 gastric cancer cells as 61.2 and 78.9 μM [46]. Compared with this study, all the synthesized procaine compounds exhibited a greater cytotoxic effect on MKN-45 cells than procaine, while palladium complexes exhibited a better cytotoxicity than the ligands. As a study similar to our results, Halby et al. [50] reported that they synthesized the new procainamide derivatives and some of these compounds exhibited cytotoxic effects on DU-145 prostate cancer cells and HCT-116 colon cancer cells [50].

Furthermore, many metal-based drugs undergo redox processes unlike to the most of organic chemotherapeutics in the cellular environment. These cases significantly affect and modify the physicochemical properties of such complexes due to geometry, charge, and reactivity. Hence, the knowledge of the redox potential can be crucial for the understanding of the mode of action underlying the anticancer activity of metal compounds [47,48]. It has been reported that, compared to meta- and *para*-counterparts, the presence of functional groups in the ortho position of ligand attached to palladium may increase cytotoxic ability. In the L^1-Pd and L^2-Pd, palladium is attached to the hydroxyl group in

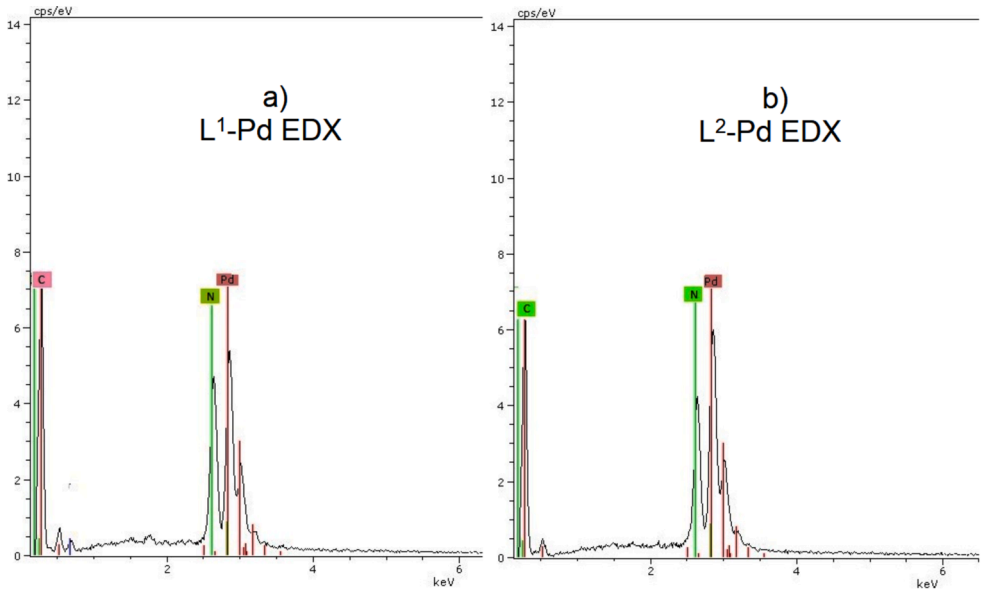

Fig. 5. The EDX pictograms of obtained complexes.

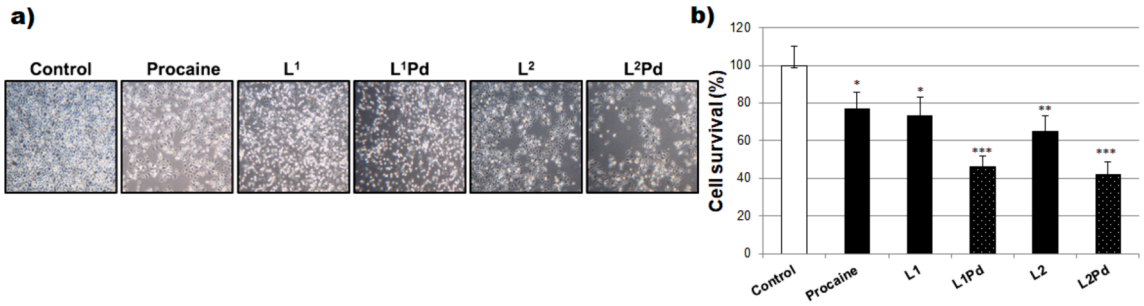

Fig. 6. The effect of procaine derivatives and the palladium complexes in MKN-45 gastric cancer cells. a) Cell morphological changes after treatment with IC_{50} doses of procaine derivatives and its palladium complexes in MKN-45 cell lines for 24 h. b) Graphical illustration of % cell survival rate of MKN-45 cells after treatment with IC_{50} doses of procaine derivatives and its palladium complexes.

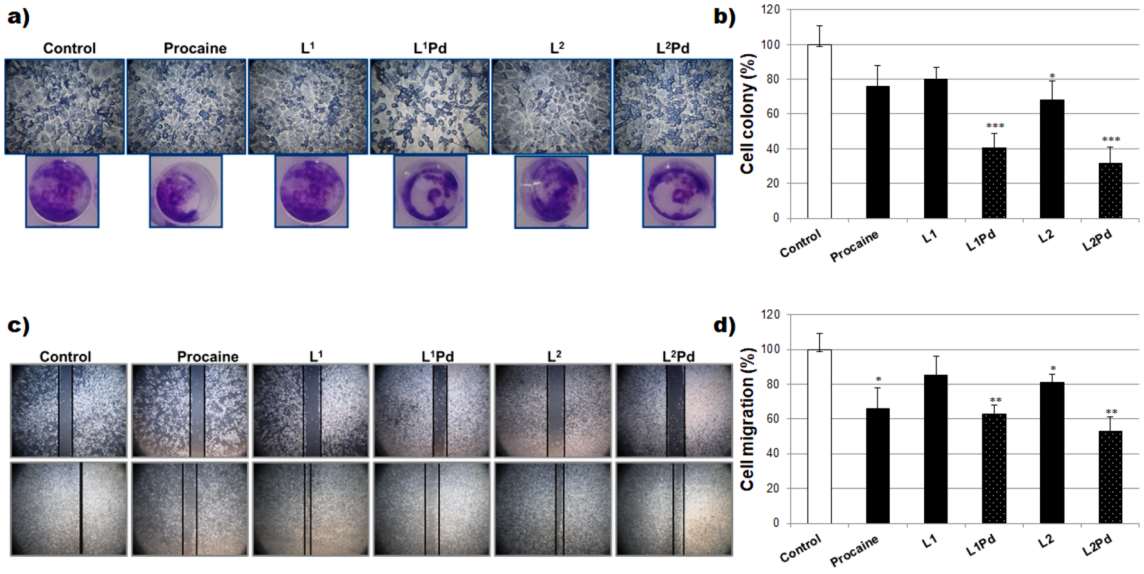

Fig. 7. Effects of procaine derivatives and its palladium complexes on cell migration in MKN-45 cells. a) Colony formation assay in MKN-45 cells. Cells were treated with IC_{50} doses of procaine derivatives and their palladium complexes and were cultured for 14 days and were stained with crystal violet. Colonies showed as overview images (up) and detailed images.

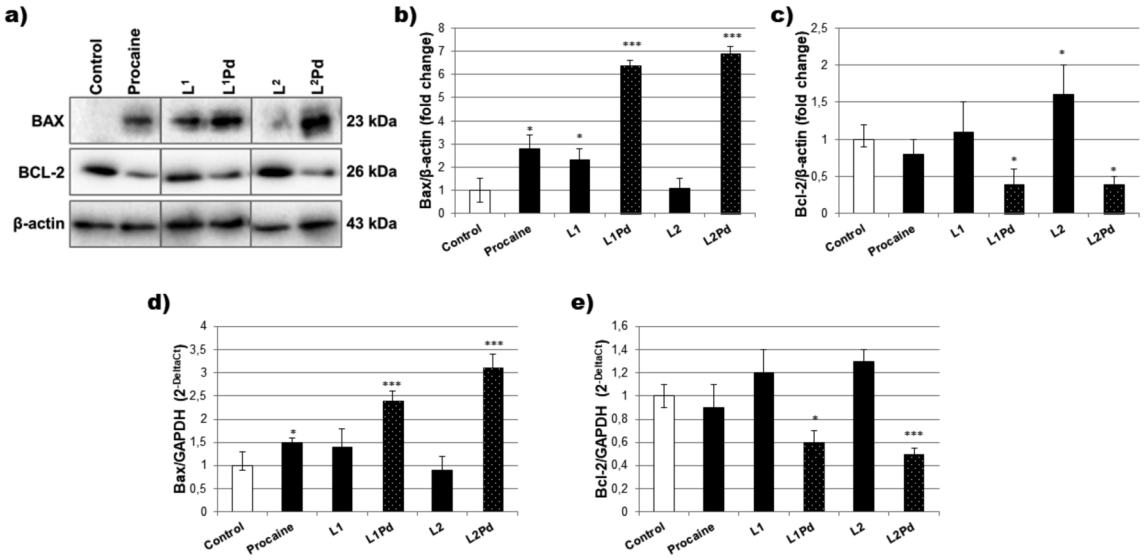

Fig. 8. Effects of procaine derivatives and its palladium complexes on apoptotic proteins in MKN-45 gastric cancer cells. a) Western blot analysis of expression levels of Bax and Bcl-2 proteins in IC_{50} doses of procaine, ligands and palladium complexes in MKN-45 cells. Each protein band was normalized to the intensity of β-actin used. b) Western blot densitometry analysis of the ratio of Bax/β-actin protein expression levels in MKN-45 cells (*$p < 0.05$, ***$p < 0.001$, compared to control cells) for the three biological replicates within each group. c) Western blot densitometry analysis of the ratio of Bcl-2/β-actin protein expression levels in MKN-45 cells. (*$p < 0.05$, compared to control cells) for the three biological replicates within each group. d-e) Effects of procaine, ligands and palladium complexes on Bax and Bcl-2 gene expression in MKN-45 cells (*$p < 0.05$ and ***$p < 0.001$ compared to control in PC3 cells).

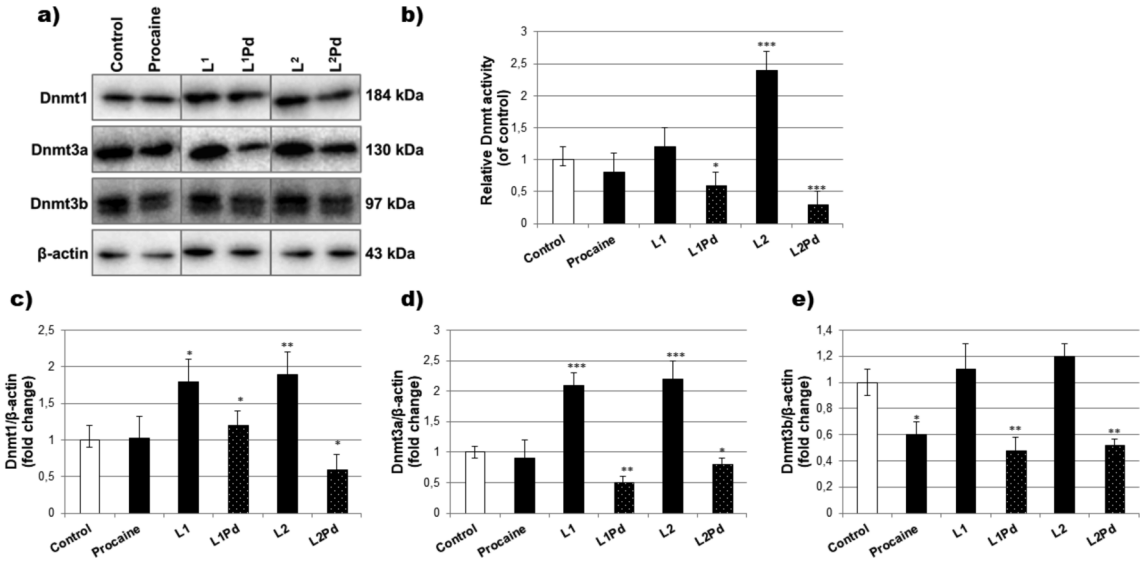

Fig. 9. Methylation status of MKN-45 cells after exposure to procaine derivatives and its palladium complexes using western blot and methylation analysis of DNMT1, 3a/3b. A) Western blot bands of expression levels of DNMT1, 3a/b proteins in procaine derivatives and its palladium complexes (10 μM) for 24 h treatment in MKN-45 cells. Each protein band was normalized to the intensity of β-actin used. B) Effects of procaine, ligands and palladium complexes on DNMT enzyme activity (10 μM) for 24 h treatment in MKN-45 cells C) Western blot densitometry analysis of the ratio of DNMT1/β-actin protein expression levels in MKN-45 cells. (*$p < 0.05$, **$p < 0.01$, compare to control cells) for the three biological replicates within each group. D) Western blot densitometry analysis of the ratio of DNMT3a/β-actin protein expression levels in MKN-45 cells. (*$p < 0.05$, **$p < 0.01$, ***$p < 0.001$ compared to control cells) for the three biological replicates within each group. E) Western blot densitometry analysis of the ratio of DNMT3b/β-actin protein expression levels in MKN-45 cells. (**$p < 0.01$ compare to control cells) for the three biological replicates within each group.

the ortho position from salicylaldehyde with a coordination bond. For this reason, palladium complexes exhibited better cytotoxic effects in MKN45 cells than ligands.

The cytotoxicity parameters for MKN-45 cells, in terms of IC_{50} obtained after 24 h of exposure, are listed in Table 1.

3.3. Clonogenic and wound healing assay

First approach was the examination of the effects of procaine derivatives and their palladium complexes treatment on colony formation ability against MKN-45 cells. As shown Fig. 7a, the number of colonies are reduced by the exposure of MKN-45 cells with procaine, L^1, L^1-Pd, L^2 and L^2-Pd,. Especially in IC_{50} doses of L^1-Pd and L^2-Pd, colony development drastically decreased by 40% and 35%, respectively, compared

Table 1
The IC_{50} values of MKN-45 cells treated with procaine derivatives and the Palladium complexes.

Compounds	IC_{50} Values (μM)
Procaine	35.06 ± 3.01
L^1	13.19 ± 1.07
L^1-Pd	10.21 ± 2.21
L^2	13.15 ± 1.06
L^2-Pd	10.79 ± 1.48

to the control group (Fig. 7b). Similar to colony formation assay, treatment of MKN-45 cells with procaine, L^1, L^1-Pd, L^2 and L^2-Pd resulted in a significant decrease in cell motility in the scratch area compared to control after 24 h of scratch formation (Fig. 7c). In Fig. 7d, L^1-Pd and L^2-Pd respectively showed 63% and %56 inhibition of tumor cell motility through wound healing in MKN-45 cells. The data suggested that procaine, L^1, L^1-Pd, L^2, and L^2-Pd diminish the metastasis effect of MKN-45 gastric cancer cells and highly effective in inhibiting migration. Our results indicate that the novel synthesized procaine derivatives and their palladium complexes had an inhibitory effect on colony formation and wound healing on MKN-45 cells which would have the effect on reducing metastasis of cancers such as gastric cancer.

3.4. Apoptotic proteins and genes expression

Apoptosis is an efficient pathway for the control of cancer cells and there are two different pathways for this to occur, based on the initiator signal occurring within the cells. The extrinsic pathway is initiated in the cell membrane, through death receptors, while the intrinsic pathway is controlled through the Bcl-2 protein family and affects the permeability of the mitochondrial outer membrane. For apoptosis to occur, it is important that drug molecules are able to enter the cell and activate the mitochondrial pathway [49]. Measurement of the expression levels of Bax and Bcl-2 are most commonly used as apoptosis markers. Increased levels of Bcl-2 expression in cancer cells prevent apoptosis and lead to tumor progression, while a decrease in Bcl-2 and an increase in Bax expression induce cell death and eliminate tumor cells [50–52]. In order to determine apoptotic effects of procaine, ligands, and palladium complexes on MKN-45 cells, we examined to expression levels of anti-apoptotic protein Bcl-2 and pro-apoptotic protein Bax (Fig. 8a). The obtained data showed that for the procaine, L^1-Pd, and L^2-Pd the expression level of pro-apoptotic protein Bax was increased, while the expression of anti-apoptotic protein Bcl-2 was dramatically reduced after 24 h of treatment. However, the levels of Bcl-2 expression in L^1 and L^2 treated MKN-45 cells increased as compared to the control group (Fig. 8b and Fig. 8c). On the other hand, by looking at gene expression data, the findings indicated that the expression levels of Bax (pro-apoptotic gene) were increased significantly (Fig. 8d) in MKN-45 cells treated with L^1-Pd and L^2-Pd while the expression levels of Bcl-2 (anti-apoptotic gene) were notably decreased relative to the control (Fig. 8e). The results clearly showed that especially L^1-Pd and L^2-Pd complexes induced cell death by triggering apoptotic pathways. In a similar study, Valentini et al. stated that palladium complexes of Curcumin activate apoptosis by increasing Bax levels and decreasing Bcl-2 levels in LNCaP, PC3 and DU145 prostate cancer cells [53].

3.5. DNMT activity

One of the current approaches in cancer treatment is the development of DNMT inhibitors. Recently, scientists have studied on the development of DNMT inhibitors [50,54,55]. DNMT1, DNMT3a and DNMT3b are the main enzymes responsible for methylation in mammals [56]. In this regard, we observed DNMT cellular enzymatic activity at the IC_{50} concentration of the test compounds. The examination of DNMT enzyme activity values revealed that in the case of L^1-Pd and L^2-Pd lower activities are detected and activity increase are obtained by the treatment of the L^1 and L^2 compared to control (Fig. 9b). The effects of procaine derivatives and the palladium complexes on the levels of DNMT protein expression were performed *via* western blotting using specific antibodies against DNMT1, DNMT3a, and DNMT3b (Fig. 9a). Our findings showed that the expression level of DNMT1, DNMT3a and DNMT3b was decreased for the procaine, L^1-Pd and L^2-Pd while the expression level of DNMT1, DNMT3a and DNMT3b was increased for the L^1 and L^2 after 24 h of treatment (Fig. 9c, 9d and 9e). 3a and 3b have been shown in literature for various types of cancer for overexpression of DNMT1 [57,58]. In light of this information, new inhibitors that reduce the methylation activity of DNMTs are being developed in cancer treatment [7]. For this aim, Pechalrieu et al. [50] synthesized some of the novel 3-halo-3-nitroflavones and stated that compounds 3a and 3b provide inhibition on DNMT and inhibition level is obtained at a micromolar concentration by the treatment of 3a. In a similar study, Pellerito et al. [59] synthesized the dibutyltin (IV) complex of caffeic acid and demonstrated that these compounds reduce protein levels of DNMT1 in MDA-MB 231 and HCT116 cells by western blot techniques [59]. Similar in this study, especially procaine, L^1-Pd and L^2-Pd significantly reduced the protein expression levels of DNMT-1,3a/3b in our study. It also shows that DNA methylation-mediated regulation of genes involved in apoptosis may be a different mechanism in cancer by escaping tumor cells from apoptosis. These changes are either hypomethylation to reactivate anti-apoptotic genes or hypermethylation to suppress pro-apoptotic genes [60]. Genes involved in mitochondrial apoptosis in glioblastoma cells are associated with DNA methylation and involved in metastasis in cancer [61].

4. Conclusion

In this study, the DNMT inhibitory potential of newly synthesized procaine derivatives and their palladium complexes (L^1, L^1-Pd, L^2, and L^2-Pd) was investigated on MKN-45 cells. Consequently, in this study, MKN-45 cells treated with synthesized L^1-Pd and L^2-Pd compounds were stimulated to apoptosis by suppressing both anti-apoptotic Bcl-2 expression and inducing pro-apoptotic Bax expression. Furthermore, it was also found that the tested compounds showed an inhibitory effect on colony formation and wound healing. In addition, since the palladium complexes of the synthesized ligands provide inhibition on DNMT1, 3a/3b enzymes, the activation of tumor suppressor genes was triggered by preventing DNA methylation. Therefore, this study highlights the importance of discovering and developing new drug derivatives used in the treatment of gastric cancer and sheds light on new research.

CRediT authorship contribution statement

Salih Paşa: Conceptualization, Investigation, Methodology, Formal analysis. **Omer Erdogan:** Investigation, Software, Validation, Data curation. **Ozge Cevik:** Conceptualization, Resources, Investigation, Writing – original draft, Writing – review & editing.

Declaration of Competing Interest

The authors declare that they have no known competing financial interests or personal relationships that could have appeared to influence the work reported in this paper.

Acknowledgements

We thank ADU-BILTEM for providing laboratory and facility support for our research. This work was supported by the Aydin Adnan Menderes University Scientific Research Foundation with the project number TPF-20012 to Dr. Ozge Cevik.

Appendix A. Supplementary material

Supplementary data to this article can be found online at https://doi.org/10.1016/j.inoche.2021.108846.

References

[1] D. Katz, E. Ito, K.S. Lau, J.D. Mocanu, C. Bastianutto, A.D. Schimmer, F.-F. Liu, Increased efficiency for performing colony formation assays in 96-well plates: novel applications to combination therapies and high-throughput screening, Biotechniques 44 (2S) (2008) ix–xiv.

[2] L.G. Rodriguez, X. Wu, J.-L. Guan, Wound-healing assay, in, Cell Migration, Springer (2005) 23–29.

[3] S.R. Bohl, L. Bullinger, F.G. Rücker, Epigenetic therapy: azacytidine and decitabine in acute myeloid leukemia, J Expert Review of Hematology 11 (5) (2018) 361–371.

[4] A. Minkovsky, A. Sahakyan, G. Bonora, R. Damoiseaux, E. Dimitrova, L. Rubbi, M. Pellegrini, C.G. Radu, K. Plath, chromatin, A high-throughput screen of inactive X chromosome reactivation identifies the enhancement of DNA demethylation by 5-aza-2′-dC upon inhibition of ribonucleotide reductase, Epigenetics 8 (2015) 1–17.

[5] M.-P. Ramos, N.A. Wijetunga, A.S. McLellan, M. Suzuki, J.M. Greally, chromatin, DNA demethylation by 5-aza-2′-deoxycytidine is imprinted, targeted to euchromatin, and has limited transcriptional consequences, Epigenetics 8 (2015) 1–18.

[6] A.K. Giri, T.J.F.i.p. Aittokallio, DNMT inhibitors increase methylation in the cancer genome 10 (2019) 385.

[7] J. Gao, L. Wang, J. Xu, J. Zheng, X. Man, H. Wu, J. Jin, K. Wang, H. Xiao, S. Li, Aberrant DNA methyltransferase expression in pancreatic ductal adenocarcinoma development and progression, J Exp Clin Cancer Res 32 (2013) 1–10.

[8] C. Mathilde, P. Romain, H. Eric, M.V. Francois, C. Pierre-Francois, DNMT Inhibitors in Cancer, Current Treatments and Future Promising Approach: Inhibition of Specific DNMT-Including Complexes, Epigenetic Diagnosis & Therapy (Discontinued) 1 (2015) 37–48.

[9] M. Cheray, R. Pacaud, E. Hervouet, F.M. Vallette, P.-F. Cartron, DNMT inhibitors in cancer, current treatments and future promising approach: Inhibition of specific DNMT-Including complexes, Epigenetic Diagnosis Therapy 1 (2015) 37–48.

[10] J. Du, L.M. Johnson, S.E. Jacobsen, D. Patel, DNA methylation pathways and their crosstalk with histone methylation, Nat Rev Mol Cell Biol 16 (2015) 519.

[11] C. Gros, J. Fahy, L. Halby, I. Dufau, A. Erdmann, J.-M. Gregoire, F. Ausseil, S. Vispé, P.B. Arimondo, DNA methylation inhibitors in cancer: recent and future approaches, Biochimie 94 (2012) 2280–2296.

[12] O. Castillo-Aguilera, P. Depreux, L. Halby, P. Arimondo, L. Goossens, DNA methylation targeting: the DNMT/HMT crosstalk challenge. Biomolecules 7, E3 Medline, (2017).

[13] A. Gnyszka, Z. Jastrzębski, S. Flis, DNA methyltransferase inhibitors and their emerging role in epigenetic therapy of cancer, Anticancer Res 33 (2013) 2989–2996.

[14] A.R. Kapdi, I.J. Fairlamb, Anti-cancer palladium complexes: a focus on PdX 2 L 2, palladacycles and related complexes, Chem Soc Rev 43 (2014) 4751–4777.

[15] M. Carreira, R.n. Calvo-Sanjuán, M. Sanaú, I. Marzo, M. Contel, Organometallic palladium complexes with a water-soluble iminophosphorane ligand as potential anticancer agents, Organometallics 31 (2012) 5772–5781.

[16] R. Czarnomysy, A. Surażyński, A. Muszynska, A. Gornowicz, A. Bielawska, K. Bielawski, A novel series of pyrazole-platinum (II) complexes as potential anti-cancer agents that induce cell cycle arrest and apoptosis in breast cancer cells, J Enzyme Inhib Med Chem 33 (2018) 1006–1023.

[17] B. Brueckner, F. Lyko, DNA methyltransferase inhibitors: old and new drugs for an epigenetic cancer therapy, Trends Pharmacol Sci 25 (2004) 551–554.

[18] S. Castellano, D. Kuck, M. Sala, E. Novellino, F. Lyko, G.J.J.o.m.c. Sbardella, Constrained analogues of procaine as novel small molecule inhibitors of DNA methyltransferase-1, 51 (2008) 2321-2325.

[19] M. Joshi, S.N. Rajpathak, S.C. Narwade, D. Deobagkar, d. design, Ensemble-Based Virtual Screening and Experimental Validation of Inhibitors Targeting a Novel Site of Human DNMT 1, Chemical Biology 88 (2016) 5–16.

[20] Y.C. Li, Y. Wang, D.D. Li, Y. Zhang, T.C. Zhao, C.F. Li, Procaine is a specific DNA methylation inhibitor with anti-tumor effect for human gastric cancer, J Cell Biochem 119 (2018) 2440–2449.

[21] H. Sabit, M.B. Samy, O.A. Said, M.M. El-Zawahri, Procaine induces epigenetic changes in HCT116 colon cancer cells, Genetics Research International, 2016 (2016) 1-7.

[22] M. Tang, W. Xu, Q. Wang, W. Xiao, R. Xu, Potential of DNMT and its epigenetic regulation for lung cancer therapy, Curr Genomics 10 (2009) 336–352.

[23] N.I. Krikova, S.N. Shcherbak, I.A. Savich, Synthesis and study of the properties of some azomethine compounds, Chem Heterocycl Compd 3 (4) (1967) 249–252.

[24] E. Trailina, L. Gul'chenko, I. Savin, The bacteriostatic activity of certain azomethine derivatives of amino and sulfonic acids, Pharm Chem J 6 (1972) 577–579.

[25] Li Jie, Liu Hongyan, Wang Shujun, Fabrication of ABS/PC alloy hollow microspheres via water/oil/water emulsion solvent evaporation, Mater Lett 65 (17-18) (2011) 2696–2699.

[26] A. Samanta, D.K. Chanda, P.S. Das, J. Ghosh, A.K. Mukhopadhyay, A. Dey, Synthesis of nano calcium hydroxide in aqueous medium, J Am Ceram Soc 99 (2016) 787–795.

[27] I.R. Hill, I.W. Levin, Vibrational spectra and carbon–hydrogen stretching mode assignments for a series of n-alkyl carboxylic acids, J Chem Phys 70 (1979) 842–851.

[28] O. Erdogan, M. Abbak, G.M. Demirbolat, F. Birtekocak, M. Aksel, S. Pasa, O. Cevik, Green synthesis of silver nanoparticles via Cynara scolymus leaf extracts: The characterization, anticancer potential with photodynamic therapy in MCF7 cells, PLoS ONE 14 (2019) 1–15.

[29] O. Cevik, F.A. Turut, H. Acidereli, S. Yildirim, Cyclosporine-A induces apoptosis in human prostate cancer cells PC3 and DU145 via downregulation of COX-2 and upregulation of TGFβ, Turkish J Biochem 44 (2019) 47–54.

[30] N. Hosseinzadeh, T. Shomali, S. Hosseinzadeh, F. Raouf Fard, J. Jalaei, M. Fazeli, Cytotoxic activity of Ferula persica gum essential oil on murine colon carcinoma (CT26) and Vero cell lines, Journal of Essential Oil Research, (2020) 1-9.

[31] O. Cevik, D. Li, E. Baljinnyam, D. Manvar, E.M. Pimenta, G. Waris, B.J. Barnes, N. Kaushik-Basu, Interferon regulatory factor 5 (IRF5) suppresses hepatitis C virus (HCV) replication and HCV-associated hepatocellular carcinoma, J Biol Chem 292 (2017) 21676–21689.

[32] O. Cevik, H. Acidereli, F.A. Turut, S. Yildirim, C. Acilan, Cabazitaxel exhibits more favorable molecular changes compared to other taxanes in androgen-independent prostate cancer cells, J Biochem Mol Toxicol 34 (2020) 1–12.

[33] M. Erşahin, Ö. Çevik, D. Akakın, A. Şener, L. Özbay, B.C. Yegen, G. Şener, Montelukast inhibits caspase-3 activity and ameliorates oxidative damage in the spinal cord and urinary bladder of rats with spinal cord injury, Prostaglandins Other Lipid Mediat 99 (2012) 131–139.

[34] P. Smith, R. Krohn, G. Hermanson, A. Mallia, F. Gartner, M. Provenzano, E. Fujimoto, N. Goeke, B. Olson, D. Klenk, Measurement of protein using bicinchoninic acid, Anal Biochem 150 (1985) 76–85.

[35] O. Cevik, Z. Adiguzel, A.T. Baykal, G. Somay, A. Sener, The apoptotic actions of platelets in acute ischemic stroke, Mol Biol Rep 40 (2013) 6721–6727.

[36] M. Yusuf, S. Thakur, Synthesis, characterization & in vitro antimicrobial-antioxidant studies of novel N,1-diphenyl-4,5-dihydro-1H-1,2,4-triazol-3-amine derivatives, J Heterocycl Chem 56 (2019) 3403–3413.

[37] N.M. Aghatabay, M. Somer, M. Senel, B. Dulger, F. Gucin, Raman, FT-IR, NMR spectroscopic data and antimicrobial activity of bis [μ2-(benzimidazol-2-yl)-2-ethanethiolato-N, S, S-chloro-palladium (II)] dimer,[(μ_2-$_C$H2$_C$H2NHN$_C$C$_6$H4) PdCl] 2.C$_2$H5OH complex, Eur J Med Chem 42 (2007) 1069–1075.

[38] H. Kabeer, S. Hanif, A. Arsalan, S. Asmat, H. Younus, M. Shakir, Structural-Dependent N, O-Donor Imine-Appended Cu(II)/Zn(II) Complexes: Synthesis, Spectral, and in Vitro Pharmacological Assessment, ACS Omega 5 (2020) 1229–1245.

[39] I. Georgieva, N. Mintcheva, N. Trendafilova, M. Mitewa, IR study of the N, N′, N″-triphenylguanidine and its imine nitrogen coordinated Pd (II) complexes, Vib Spectrosc 27 (2001) 153–164.

[40] S. Chen, M. Pudukudy, Z. Yue, H. Zhang, Y. Zhi, Y. Ni, S. Shan, Q. Jia, Nonmetal Schiff-Base Complex-Anchored Cellulose as a Novel and Reusable Catalyst for the Solvent-Free Ring-Opening Addition of CO_2 with Epoxides, Ind Eng Chem Res 58 (2019) 17255–17265.

[41] Hua Zhang, Peiwen Liu, Xinwen Peng, Shuiliang Chen, Kai Zhang, Interfacial Synthesis of Cellulose-Derived Solvent-Responsive Nanoparticles via Schiff Base Reaction, ACS Sustainable Chem Eng 7 (19) (2019) 16595–16603.

[42] Salih Pasa, Yusuf Selim Ocak, Hamdi Temel, Tahsin Kilicoglu, Synthesis, characterization and catalytic behavior in the Suzuki reaction of Schiff base and its complexes and the optical properties of nickel complex used in the fabrication of a photodiode, Inorg Chim Acta 405 (2013) 493–504.

[43] Hamdi Temel, Salih Pasa, Yusuf Selim Ocak, Ismail Yilmaz, Serpil Demir, Ismail Ozdemir, Synthesis, characterization, electrochemical behaviors and applications in the Suzuki-Miyaura cross-coupling reactions of $N_2S_2O_2$ thio Schiff base ligand and its Cu(II), Co(III), Ni(II), Pd(II) complexes and their usage in the fabrication of organic–inorganic hybrid devices, Synth Met 161 (23-24) (2012) 2765–2775.

[44] V. Kettmann, D. Košťálová, S. Jantova, M. Čerňáková, In vitro cytotoxicity of berberine against HeLa and L1210 cancer cell lines, Die Pharmazie-An Int J Pharm Sci 59 (2004) 548–551.

[45] A Senff-Ribeiro, A Echevarria, E F Silva, C R C Franco, S S Veiga, M B M Oliveira, Cytotoxic effect of a new 1, 3, 4-thiadiazolium mesoionic compound (MI-D) on cell lines of human melanoma, Br J Cancer 91 (2) (2004) 297–304.

[46] M. Tanaka, H. Kataoka, S. Yano, H. Ohi, K. Kawamoto, T. Shibahara, T. Mizoshita, Y. Mori, S. Tanida, T. Kamiya, Anti-cancer effects of newly developed chemotherapeutic agent, glycoconjugated palladium (II) complex, against cisplatin-resistant gastric cancer cells, BMC cancer 13 (2013) 1–9.

[47] Ehsan Zareian Jahromi, Adeleh Divsalar, Ali Akbar Saboury, Sara Khaleghizadeh, Hassan Mansouri-Torshizi, Irena Kostova, Palladium complexes: new candidates for anti-cancer drugs, J Iran Chem Soc 13 (5) (2016) 967–989.

[48] U. Jungwirth, C.R. Kowol, B.K. Keppler, C.G. Hartinger, W. Berger, P. Heffeter, Anticancer activity of metal complexes: involvement of redox processes, Antioxid Redox Signal 15 (2011) 1–91.

[49] J. Armstrong, Mitochondrial medicine: pharmacological targeting of mitochondria in disease, Br J Pharmacol 151 (2007) 1154–1165.

[50] D. Pechalrieu, D. Dauzonne, P.B. Arimondo, M. Lopez, Synthesis of novel 3-halo-3-nitroflavanones and their activities as DNA methyltransferase inhibitors in cancer cells, Eur J Med Chem 186 (2020), 111829.

[51] D. Korbakis, A. Scorilas, Quantitative expression analysis of the apoptosis-related genes BCL2, BAX and BCL2L12 in gastric adenocarcinoma cells following treatment with the anticancer drugs cisplatin, etoposide and taxol, Tumor Biology 33 (2012) 865–875.

[52] F. Shabani, M. Mahdavi, M. Imani, M. Hosseinpour-Feizi, N. Gheibi, Calprotectin (S100A8/S100A9)-induced cytotoxicity and apoptosis in human gastric cancer AGS cells: Alteration in expression levels of Bax, Bcl-2, and ERK2, Hum Exp Toxicol 39 (2020) 1031–1045.
[53] A. Valentini, F. Conforti, A. Crispini, A. De Martino, R. Condello, C. Stellitano, G. Rotilio, M. Ghedini, G. Federici, S. Bernardini, Synthesis, oxidant properties, and antitumoral effects of a heteroleptic palladium (II) complex of curcumin on human prostate cancer cells, J Med Chem 52 (2009) 484–491.
[54] L. Halby, C. Champion, C. Sénamaud-Beaufort, S. Ajjan, T. Drujon, A. Rajavelu, A. Ceccaldi, R. Jurkowska, O. Lequin, W.G. Nelson, Rapid synthesis of new DNMT inhibitors derivatives of procainamide, ChemBioChem 13 (2012) 157–165.
[55] A.S. Newton, J.C. Faver, G. Micevic, V. Muthusamy, S.N. Kudalkar, N. Bertoletti, K. S. Anderson, M.W. Bosenberg, W.L. Jorgensen, Structure-Guided Identification of DNMT3B Inhibitors, ACS Med Chem Lett 11 (2020) 971–976.
[56] H. Kim, J. Kim, E. Chie, P. DaYoung, I. Kim, I. Kim, DNMT (DNA methyltransferase) inhibitors radiosensitize human cancer cells by suppressing DNA repair activity, Radiation oncology 7 (2012) 1–10.
[57] Zelin Jin, Yun Liu, DNA methylation in human diseases, Genes & Diseases 5 (1) (2018) 1–8.
[58] I. Girault, S. Tozlu, R. Lidereau, I. Bièche, Expression analysis of DNA methyltransferases 1, 3A, and 3B in sporadic breast carcinomas, Clin Cancer Res 9 (2003) 4415–4422.
[59] C. Pellerito, O. Morana, F. Ferrante, G. Calvaruso, A. Notaro, S. Sabella, T. Fiore, Synthesis, chemical characterization, computational studies and biological activity of new DNA methyltransferases (DNMTs) specific inhibitor, Epigenetic regulation as a new and potential approach to cancer therapy, J inorganic biochem 150 (2015) 18–27.
[60] G. Gopisetty, K. Ramachandran, R. Singal, DNA methylation and apoptosis, Mol Immunol 43 (11) (2006) 1729–1740.
[61] E. Hervouet, F. Vallette, P. Cartron, Impact of the DNA methyltransferases expression on the methylation status of apoptosis-associated genes in glioblastoma multiforme, Cell death & disease, 1 (2010) 1-9.